Electronic Supplementary Material (ESI) for Physical Chemistry Chemical Physics.
This journal is © the Owner Societies 2017

Supporting information of:

Ultrafast exciton dynamics in 2D in-plane hetero-nanostructures: delocalization and charge transfer

Elsa Cassette, Silvia Pedetti, Benoît Mahler, Sandrine Ithurria-L'huillier,

Benoît Dubertret and Gregory D. Scholes

Table of content:

1. **Instrumentation (structural characterization, steady state spectroscopy and time-resolved photoluminescence)**

- Transmission electron microscopy (TEM) measurements were performed on a JEOL 2010 microscope working at 200 kV and mounted with a Gatan camera.

- Absorption spectra were performed on the UV-visible-NIR spectrophotometers Cary 5E of Varian or Cary 6000i of Agilent equipped with an integrating sphere. All the nanoplatelet samples were dispersed in hexane.

- Photoluminescence (PL) and photoluminescence excitation (PLE) spectra were measured with the fluorometer FCS900 of Edinburg Instruments with a visible photomultiplier Hamamatsu R928-P643 and a Xe white lamp. The samples were dispersed in hexane with a maximum absorption about 0.1 at (and above) the excitation wavelength. The spectra are corrected at the excitation (for PLE) and at the detection (for PL).

- Photoluminescence lifetimes were recorded by time-correlated single photon counting (TCSPC) on Horiba Deltaflex equipped with a pulsed laser diode at 405 nm, with a pulse duration of about 45 ps and a repetition rate set at 1.8 µs.

2. **Sample characterizations**

- CdSe nanoplatelets

For the different samples, we prepared CdSe core NPLs with a thickness of 4.5 MLs and with various lateral dimensions, as well as a CdSe NPL sample with a thickness of 5.5 MLs (Table S1). The number of monolayers n+1/2 MLs is a semi-integer as the surface is terminated by Cd- atoms in both side of the NPLs. The thickness can thus be estimated as $n*c/2+ 2*r_{Cd}$, with c, the lattice parameter of CdSe in the zinc blende crystallographic structure and r_{Cd}, the ionic radius of a Cd atom. For example 4.5 ML and 5.5 ML NPLs have respectively a thickness of about 1.4 and 1.7 nm if we do not consider any strain induced by the ligands.

	Shape	Thickness	Width (*d*)	Length (*l*)
Sample 0	rectangle	4.5 MLs	10 ± 1 nm	17 ± 2 nm
CdSe NPLs for sample 1	oval	4.5 MLs	11 ± 1 nm	17 ± 2 nm
CdSe NPLs for sample 2	rectangle	4.5 MLs	10.5 ± 1 nm	20 ± 2 nm
CdSe NPLs for sample 3	rectangle	4.5 MLs	9.0 ± 0.9 nm	17 ± 2 nm
CdSe NPLs for sample 5	rectangle	5.5 MLs	9 ± 1 nm	38 ± 3 nm

Table S1. Thickness and lateral dimensions of the CdSe NPL cores used for the different samples.

- CdSe-CdTe in-plane NPL heterostructures

The lateral dimensions of CdSe-CdTe core-crown NPLs are displayed in Table S2. The samples are schematized in Fig. S1.

	Shape	Thickness	Width (*D*)	Length (*L*)	Ratio CdSe/total
Sample 1	rectangle	4.5 MLs	13 ± 1 nm	23 ± 3 nm	150/300 nm^2
Sample 2	rectangle	4.5 MLs	11 ± 2 nm	24 ± 3 nm	200/260 nm^2
Sample 3	rectangle	4.5 MLs	12 ± 2 nm	28 ± 4 nm	150/345 nm^2
Sample 5	rectangle	5.5 MLs	15 ± 3 nm	48 ± 10 nm	325/730 nm^2

Table S2. Thickness, lateral dimensions and CdTe/CdSe ratio of CdSe-CdTe core-crown samples.

The effect of CdSe/CdTe proportion in the dynamics can be studied by comparing samples 2, 1 and 3 (CdTe proportion versus CdSe increasing). The effect of the thickness (*i.e.* of quantum confinement) is analysed by comparing samples 3 and 5 with similar CdSe/CdTe proportions.

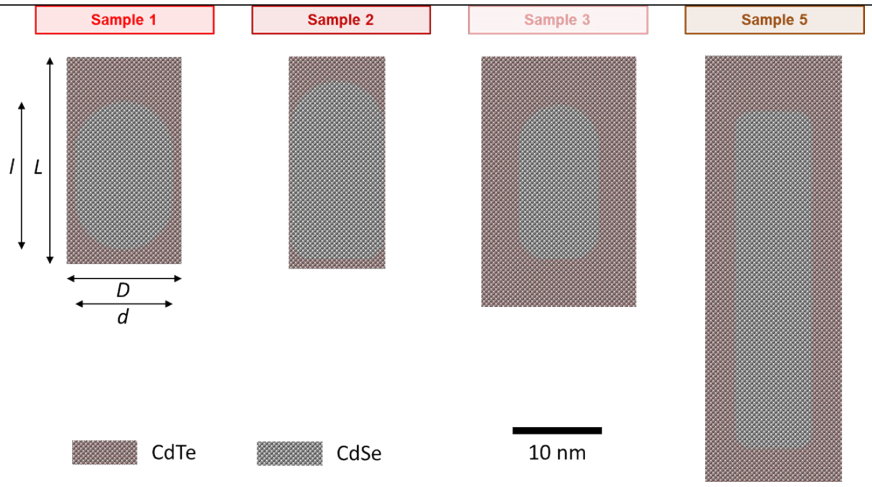

Figure S1. Schematics of CdSe-CdTe NPL samples studied. The lateral dimensions *L* x *D* (*l* x *d*) of the heterostructure (of CdSe core NPLs) are scaled proportionally to the real sizes. Samples 1, 2 and 3 have a thickness of 4.5 MLs whereas sample 5 has a thickness of 5.5 MLs.

- Optical spectra of CdSe-CdTe NPLs with 5.5 MLs (sample 5)

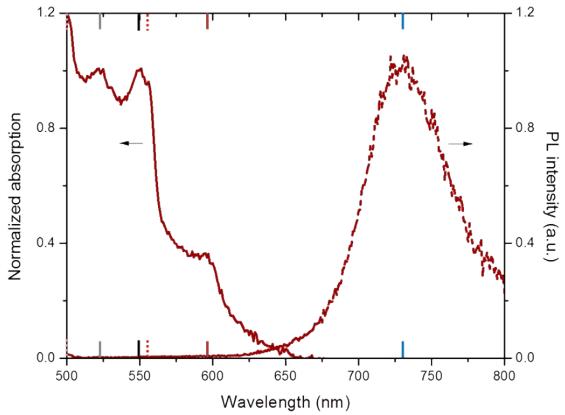

Figure S2. Normalized PL (dashed line) and PLE (full line) spectra of CdSe-CdTe NPLs of 5.5 MLs in thickness. Note: the peaks at 500 and 556 nm correspond to LX and HX transition of CdTe NPLs of 4.5 MLs, product of a secondary nucleation that appears during the CdTe crown growth.

Fig. S2, the peaks at 522 nm (2.38 eV, grey mark) and 549 nm (2.26 eV, black mark) correspond to the LX and HX transition of 5.5 ML CdSe NPLs, respectively [1]. The peak at 596 nm (2.08 eV, brown mark) that appears with the CdTe crown corresponds to the HX transition of CdTe NPLs of 5.5 MLs. We observe additional peaks at 500 and 556 nm in the absorption spectrum due to the presence of CdTe NPLs of 3.5 MLs that have nucleated on the side. These two peaks are absent in the PLE spectrum [2]. The PL spectrum is centered at about 735 nm (1.69 eV).

- NPL heterostructures with CdSeTe alloyed crown (sample 4)

For sample 4, a crown of an alloy CdSeTe was grown on the 4.5 ML CdSe NPLs. In the synthesis, we used for the crown about 40 % of Se and 60 % of Te. By using as zinc blende lattice parameter for CdSe and CdTe of 0.608 nm and 0.648 nm respectively, we obtain for the alloy a lattice parameter of 0.632 nm assuming a linear dependence with the Te/Se ratio.

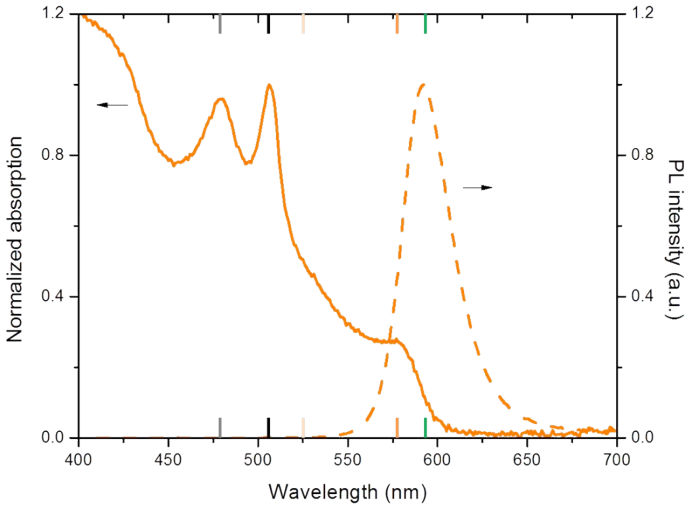

Figure S3. Photoluminescence excitation (full line, normalized at 510 nm) and emission (dashed line, normalized) spectra of CdSe-CdTeSe core-crown NPLs.

In Fig. S3, LX and HX CdSe NPL transitions are observed at 479 nm (2.59 eV, grey mark) and 506 nm (2.45 eV, black mark) respectively. CdSeTe crown growth induces a transition at 577 nm (2.15 eV, orange mark) that corresponds to the HX transition and which is well red-shifted compared to CdTe HX transition. CdSeTe LX transition cannot be resolved in this PLE spectrum but is at about 525 nm (2.36 eV, beige mark, see TA Fig. S22). The emission maximum at 593 nm (2.09 eV, green mark) is only slightly red shifted from HX CdSeTe absorption peak (Stokes shift about 60 meV, corresponding to about the half of the PL full width at half maximum).

3. Comparison of the absorption and PLE spectra

We studied the dependence of the photoluminescence quantum yield (PL QY) of CdSe-CdTe core-crown NPLs on the excitation wavelength. In order to do that, the PLE spectrum of the samples was superposed with the absorption spectrum (see Fig. S4 for sample 1). Thanks to the integrated sphere, the absorption spectrum has a limited contribution of scattered light and the PLE spectrum follows quite well this spectrum for the excitation wavelengths longer than about 470 nm. This means that no specific recombination pathway occurs at these longer wavelengths. In other words, excitation in CdSe or CdTe materials leads to the same final state.

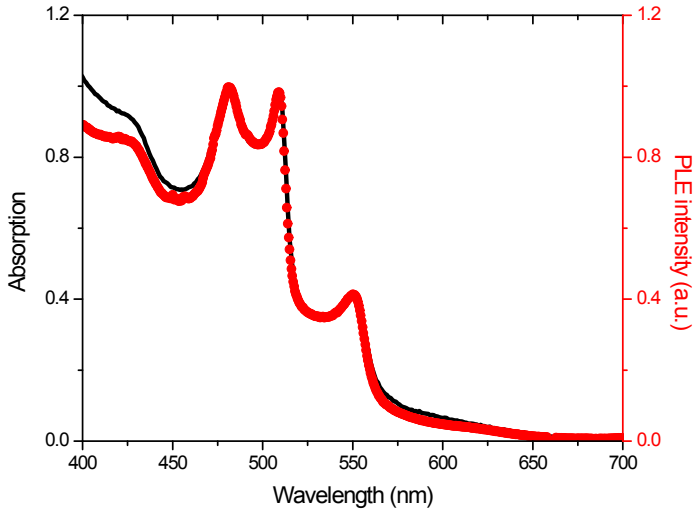

Figure S4. Absorption (normalized at 510 nm) and photoluminescence excitation (PLE, at PL maximum) spectra of CdSe-CdTe NPLs (sample 1).

4. NPL photoluminescence lifetime

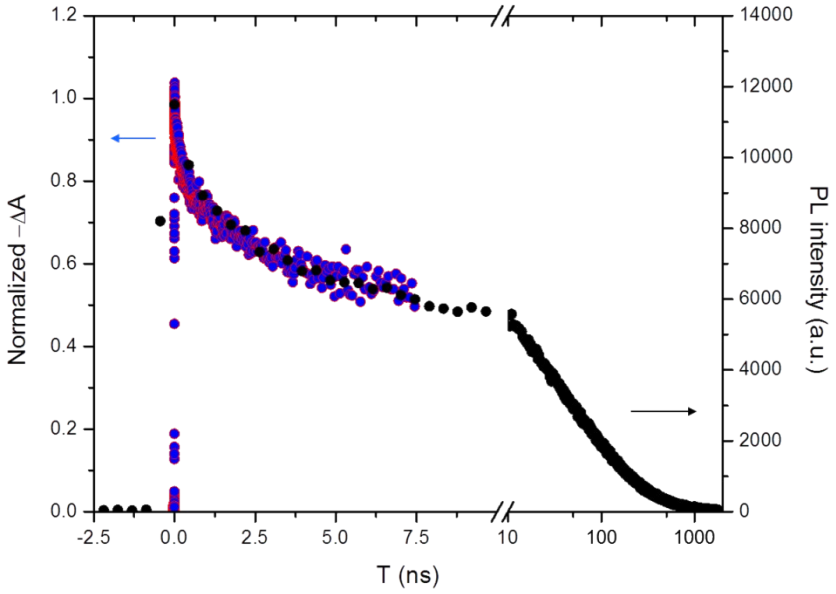

Figure S5. Photoluminescence decay at 650 nm of CdSe-CdTe NPLs (sample 1, black dots) superposed with long time TA (bleach at 630 nm after excitation at 550 nm, blue dots).

The long time dynamics at 630 nm of CdSe-CdTe NPLs in transient absorption follows the PL decay at 650 nm (Fig. S5). The state involved in the 630 nm bleach can thus be attributed to the emitting state.

PL decay curve are slightly dependent on the emission wavelength, as can be seen in Fig. S6. The PL dynamics were fitted with multiexponentials with time parameters ranging from few ns to few hundreds of ns (Table S3).

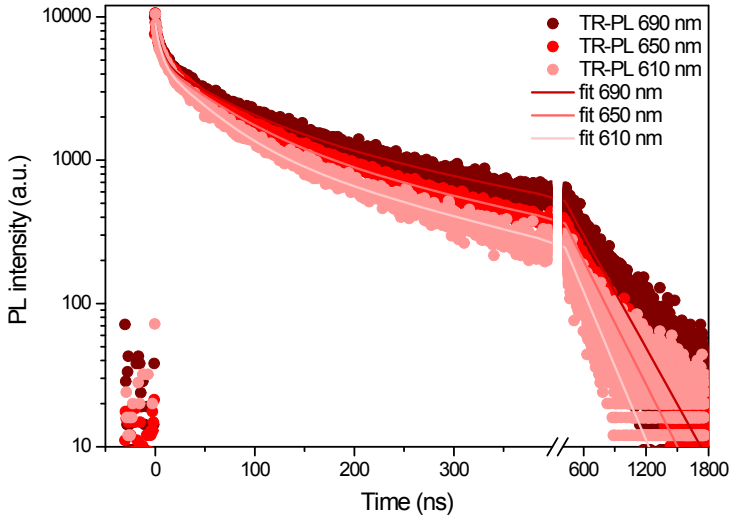

Figure S6. Wavelength dependent PL lifetime of sample 1 after excitation at 405 nm (dots). The fit parameters are shown in Table S3.

$I_{PL} = A_1 exp(-T/t_1) + A_2 exp(-T/t_2) + A_3 exp(-T/t_3)$

Emission wavelength	A_1	t_1 (ns)	A_2	t_2 (ns)	A_3	t_3 (ns)	R^2
610 nm	45 %	5.27 ± 0.09	40 %	49.6 ± 0.5	15 %	251 ± 2	0.996
650 nm	43 %	5.81 ± 0.06	40 %	63.1 ± 0.4	17 %	302 ± 2	0.998
690 nm	45 %	6.0 ± 0.1	35 %	68.7 ± 0.9	20 %	332 ± 3	0.996

Table S3. Parameters used to fit the PL decay of sample 1b at three different emission wavelengths. The equation displayed on top uses three exponentials with amplitude A_i and time constant t_i. The coefficient of determination R^2 is indicated in each case.

5. 2DES setup

2D electronic spectroscopy experiments were performed on a home-built setup initially designed by D. Turner [3] and rebuilt in the new laboratory. The broadband NOPA was tuned in the green to cover the HX CdSe and HX CdTe transitions (Fig. S7). The pulse duration was about 14 fs from the FROG measurement (Fig. S8) [4]. The first coherence time t_1 was scanned from -70 (nonrephasing signal at negative time delay) to +70 fs (rephasing at positive time delay) by step of 0.2 fs and we measured 2D spectra for waiting times (pump-probe time) t_2 from 0 to about 450 fs, by step of 5 fs.

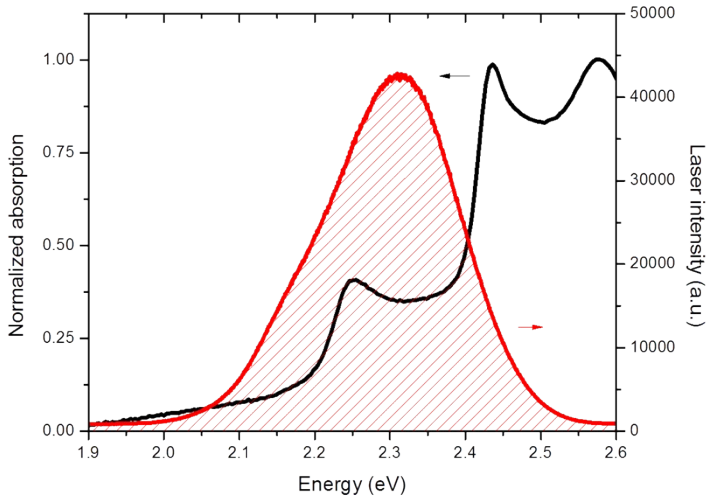

Figure S7 Broadband laser spectrum (red line) with a NOPA tuned in the green range to cover the heavy hole exciton of CdSe and CdTe in CdSe-CdTe NPLs (absorption spectrum in black).

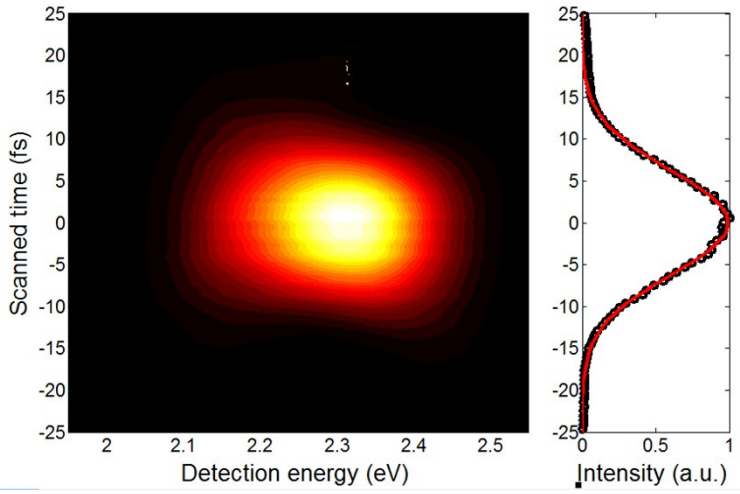

Figure S8 Measurement of the pulse duration by FROG. The Gaussian fit gives a pulse duration of about 14 fs.

6. TA setup

Transient absorption measurements were performed on a commercial transient absorption spectrometer (Helios HE-VIS-NIR 3200, Ultrafast Systems). The output of a 40 fs amplified Ti:Sapphire laser (1 kHz, Libra, Coherent) is split in two beams. One of the beam is used to pump a commercial optical parametric amplifier (OPerA Solo, Coherent), that can be broadly tuned in wavelength (UV, visible and NIR range) and that is used to excite the sample (pump pulse). The other part of the 800 nm laser beam is focused into a sapphire window to generate a white light continuum (450-800 nm) that will be used as probe. Filters were used to isolate the fundamental at 800 nm from the white light continuum.

The samples were suspended in hexane in a 2 mm thick cuvette and stirred with a magnet to avoid photocharging and sample degradation.

The transient absorption signal $\Delta A = log\left(\frac{I_0}{I}\right)$ is spectrally resolved (1.5 nm resolution) and thus by varying the pump-probe time delay we obtain a full TA map $\Delta A(T, \lambda_{det})$. Data result typically of an average of 5 to 100 scans. The resolution in the temporal steps is 8 fs (intrinsic limitation from the motorized delay stage) and the maximum time delay accessible is about 7 ns.

7. Pump and probe laser spectra

The pump laser spectra used for the experiments are displayed in Fig. S9, as well with the typical continuum white light probe.

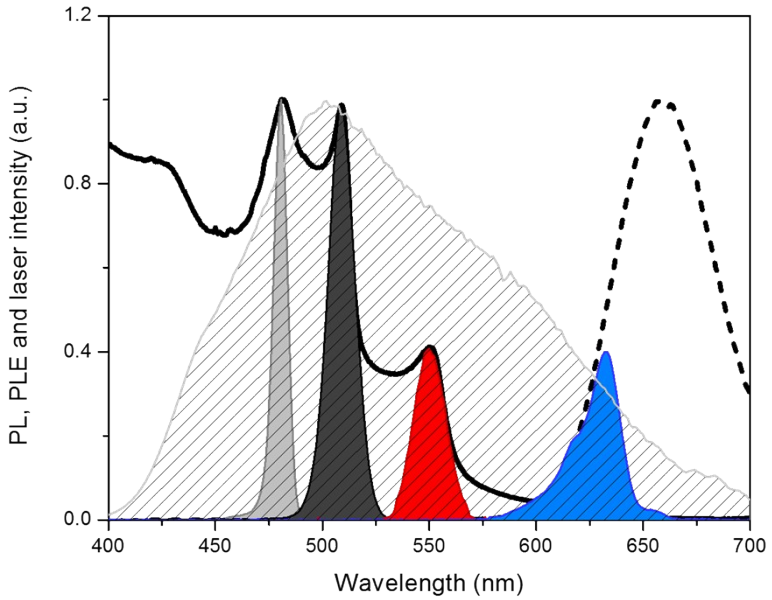

Figure S9. PL (dashed black line) and PLE (full black line) spectra of sample 1 with the typical laser spectra used for the experiments (480 nm, 510 nm, 550 nm and 630 nm). The continuum white light probe spectrum is superposed (grey hatched area).

8. Pulse duration in TA measurements

The minimum pulse duration is given by the Fourier-transform limit of the laser spectrum. In TA, we used pump pulses with a duration of about 90 fs that provide a relatively good temporal resolution without losing too much in the selectivity of the optical transitions in excitation. By assuming a Gaussian spectral envelope and a fully temporally compressed laser pulse, we can, at minimum, obtain the pulse durations given in Table S4 by using the following expression:

$$dt_{FT\ lim} = 0.44/dv$$

Where $dt_{FT\ lim}$ is the FT-limited pulse duration (FWHM) and $d\lambda$ is the FWHM of the gaussian laser spectrum in frequency.

Central wavelength	Δλ (nm)	dv (THz)	$dt_{FT\ lim}$ (fs)
480 nm	7,0	9,1	48
509 nm	15,3	17,7	25
525 nm	8,2	8,9	49
550 nm	17,7	17,5	25
586 nm	28,5	24,8	18
633 nm	20,3	15,2	29

Table S4. Excitation wavelengths used for the experiments and corresponding minimum pulse duration for a Transform-limited pulse (without any chirp).

As the pump pulse is not compressed in the TA experiment, the pump pulse present some chirp and so its duration are longer than those reported in Table S4. We did not use an autocorrelation method to measure the experimental pulse duration with accuracy. However, we can estimate them by looking at the solvent

response in the same experimental conditions and the time of the rising bleach features that should be instantaneous.

The formation of a bleach feature, when exciting at the wavelength of the corresponding optical transition, is a convolution of a Heaviside function (step function) by the pulse shape (Gaussian in general). The smoothness of the step gives information on the pulse duration. In Fig. S10, we plotted the early kinetics of the LX CdSe, HX CdSe, and HX CdTe normalized bleach when exciting at 480, 510 and 550 nm, respectively. The negative rise is similar in all case and is approximated by the following equation:

$$R(t) = -\frac{1}{2}\left[1 + erf\left(\frac{t}{\sigma\sqrt{2}}\right)\right]$$

where σ is the standard deviation corresponding to the temporal resolution, *i.e.* the FWHM of the Gaussian pulse is $dt = 2\sqrt{2ln(2)}\sigma$. We obtained $dt = 95 \pm 2$ fs.

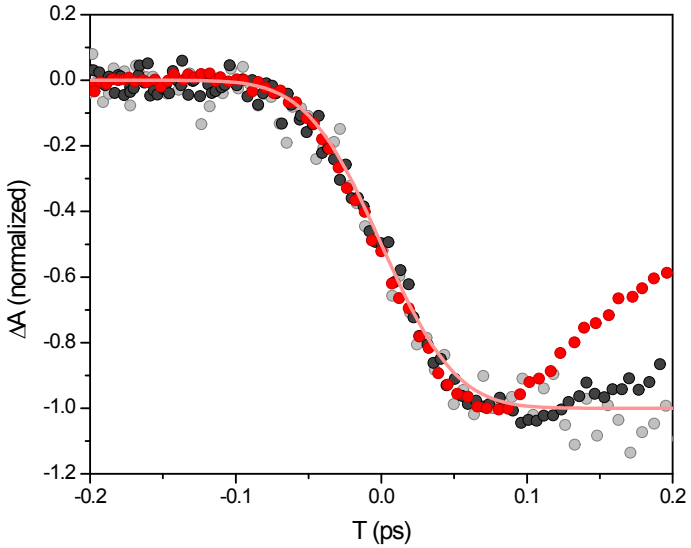

Figure S10. Early kinetics of the bleach at the excitation wavelength corresponding to the optical transition: LX CdSe for excitation at 480 nm (grey), HX CdSe for 510 nm (black) and HX CdTe for 550 nm (red). The fit for a pulse duration of 95 fs is displayed with a pink line.

In addition, fitting results with Glotaran [5] and Surface Xplorer (program with TA) gives a pump pulse duration of 50-70 fs, assuming a Gaussian envelop.

9. Power-dependent TA measurements

The average number of excitons photocreated per pulse is given by:

$$\langle N_{exc} \rangle = \frac{E_{pulse}\sigma}{\Sigma_{laser}\hbar\omega}$$

Where E_{pulse} is the energy per pulse, Σ_{laser} is the beam section, σ is the NPL cross section and $\hbar\omega$ is the absorbed photon energy.

$$E_{pulse} = \frac{\bar{P}}{RR}$$

$\bar{P}$ is the power of the pump used in the experiment, RR is the repetition rate of the laser and is 1 kHz.

$\Sigma_{laser} = \pi r^2$, with r the beam radius. The pump beam radius is larger than the probe beam radius which is about 0.1 mm and thus, at maximum, all the pump density used to excite the sample is concentrated in 3.10^{-4} cm^2. In practice, if we consider a Gaussian pulse, only about 68 % of the energy will be concentrated in the first standard deviation part of the beam.

The cross section of CdSe-CdTe NPLs depends on the volume of the nanoplatelets, the ratio of CdTe and CdSe but also of the extent of the electron wavefunction delocalisation. The latter is not directly quantifiable. However, we can estimate that the cross section of the heterostructure is in the same order of magnitude than the cross section of the CdSe core of the same thickness. For CdSe NPLs with 4.5 MLs, we have a cross section at 510 nm (2.43 eV) of about 8.10^{-14} cm^2 [6].

The estimation of the maximum average number of excitons created per pulse when excited at 510 nm with a power of 1 µW (E_{pulse} =1 nJ) is 0.45. The TA experiments were thus performed in this low power range. We note that the average power of the broadband probe was set at least 3 times smaller than the narrowband pump power.

As this calculation is an approximation, we performed several measurements at different pump powers (Fig. S11 and Table S5).

	Excitation at 480 nm							
Neutral density	3.0	2.6	2.3	2.0	1.6	1.3	1.0	0
Power (µW)	-	1.15	-	4.32	-	-	46.6	292
	Excitation at 510 nm							
Neutral density	3.0	2.6	-	2.0	-	-	1.0	0
Power (µW)	0.65	2.98	-	10.9	-	-	93.4	450
	Excitation at 550 nm							
Neutral density	3.0	2.6	-	2.0	-	-	1.0	0
Power (µW)	0.4	1.62	-	6.2	-	-	60.5	440
	Excitation at 630 nm							
Neutral density	-	2.6	2.3	2.0	1.6	1.3	1.0	0
Power (µW)	-	5.15	10.1	17.4	38.1	75.8	126	694

Table S5. Measured pump powers for each neutral density (ND) filter put in the pump path.

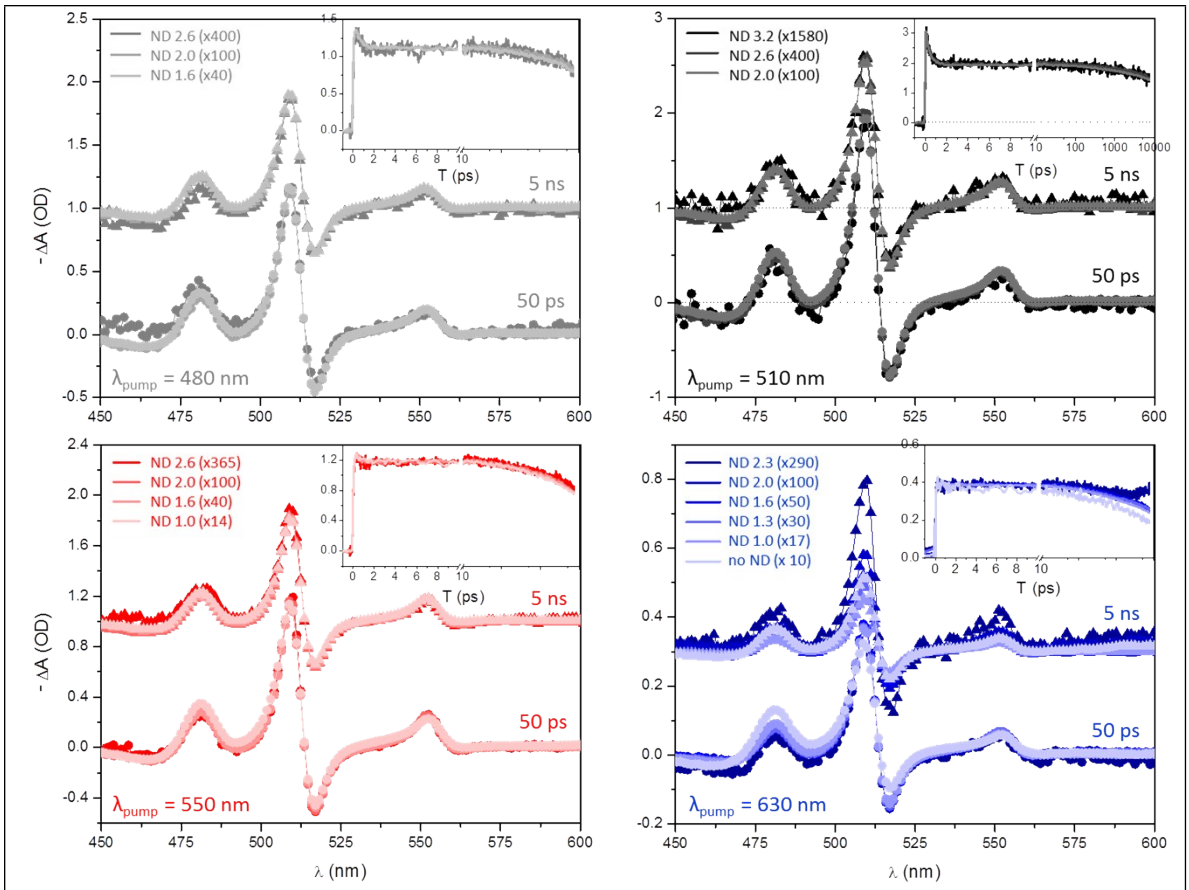

Figure S11. TA spectra (-ΔA) of CdSe-CdTe NPLs (sample 1) at 50 ps and 5 ns for four different excitation wavelengths: 480 nm (LX CdSe), 510 nm (HX CdSe), 550 nm (HX CdTe) and 630 nm (PL state). Each time, the TA spectra was multiplied by a value corresponding to the neutral density (ND) filter used to decrease the pump power. The powers values are displayed in Table S5. The TA spectra at 5 ns are translated vertically for clarity. Inset: normalised dynamics corresponding to the HX CdSe bleach.

ND	3.2	2.6	2.3	2.0	1.6	1.3	1.0	none
10^{ND}	1585	400	200	100	40	20	10	1

Table S6. Factor of multiplication that corresponds to each neutral density filter to normalise the TA spectra in case of linear dependency (low excitation density regime).

In Fig. S11, we can see the TA spectra and dynamics measured at different pump fluencies for an excitation at 480, 510 and 550 nm can be superposed by using a factor of multiplication close to the theoretical value given by the neutral density filter (Table S6). This shows that the experiments were performed at relatively low excitation fluency, in the linear regime (< 1 exciton photocreated per pulse). Some discrepancies between experimental and expected values of multiplication factor may come from a small change in the pump and probe beam overlap.

The results for excitation at 630 nm seem to slightly deviate from the linear trend. This might be due to the fact that we had to use larger pump powers and averaged much longer as the sample possess a very low oscillator strength at this wavelength.

10. Probe chirp and pump scatter corrections in TA

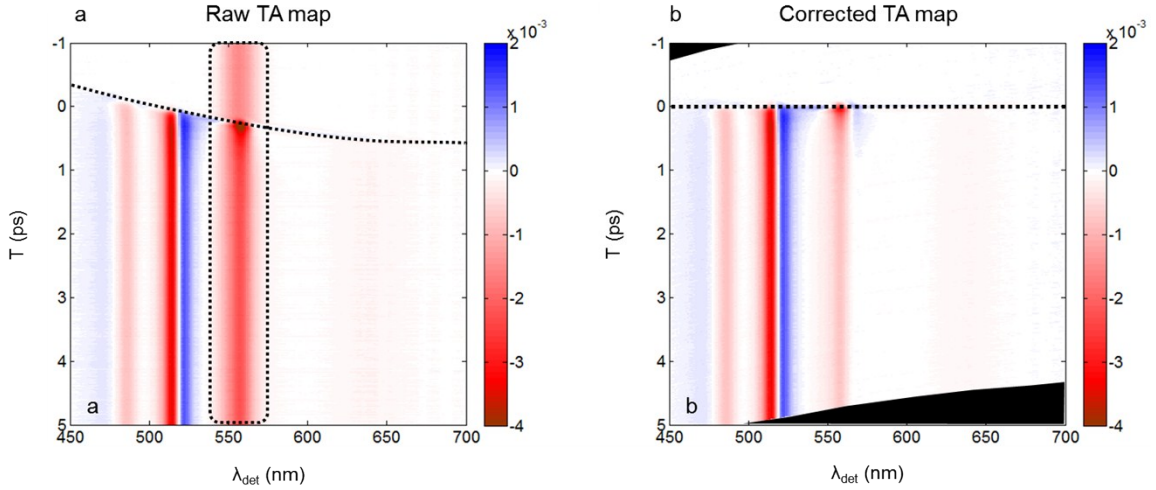

Figure S12. Example of 2D TA map (here from sample 1 when excitation at 550 nm). a. Raw data. b. Data after scatter and probe chirp corrections. The dashed line is a visual representation of the "real" time zero. The frame around 550 nm highlights the presence of some scatter at the pump wavelength. The back areas in b. correspond to the absence of data at these times/wavelengths due to the chirp correction.

The data processing were performed on Matlab. Some scatter from the pump is present in the raw TA data at the excitation (pump) wavelength, at negative and positive time (Fig. S12a). As it is not too large compared to the ΔA signal intrinsic to the sample (at $T \geq 0$ only), we directly subtract to the raw data the average of the signal at $T < -500$ fs (Fig. S12b).

In addition, the temporal dispersion in frequency (chirp) of the probe pulse was corrected in the case of the acquisition with linear time step. First the time "zero" for the different detection wavelengths was fitted with a linear or a polynomial function (order 2). Then, each row of the 2D data matrix $\Delta A(T, \lambda_{det})$ corresponding to a single detection wavelength was slightly shifted in time index by a time corresponding to the difference between the initial time "zero" and the time zero accounting from the probe chirp. The difference between the raw and corrected TA maps is displayed in Fig. S12. The probe chirp correction allows to retrieve the real TA spectrum at early times. In the case of longer times ($T > 5$ ps), the chirp can be neglected and the TA spectra are shown without chirp correction.

11. Transient spectra of samples with different lateral sizes and thickness

The time-dependent TA spectra of samples 2 and 3 which present different lateral sizes of CdSe core and CdTe crown than sample 1 is shown in Fig. S13.

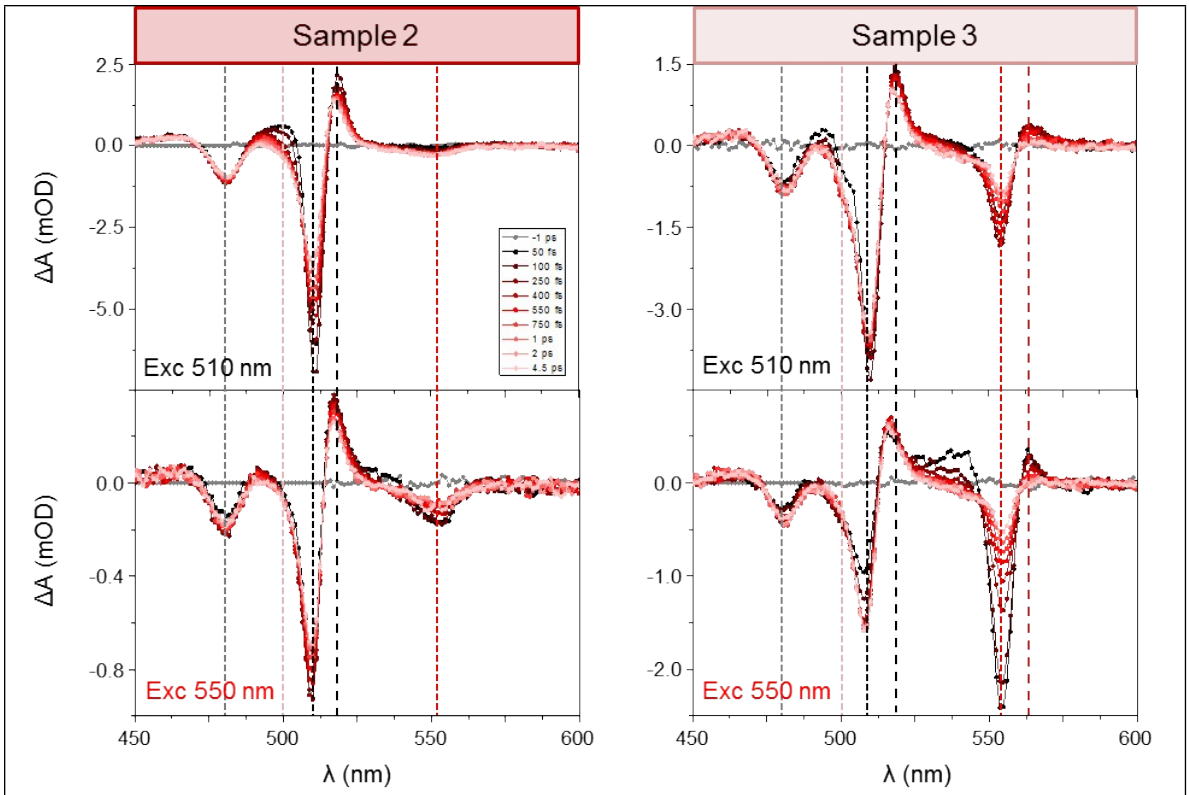

Figure S13. Transient spectra at early times of samples 2 and 3 for two different excitation wavelengths, 510 nm (HX CdSe) and 550 nm (HX CdTe).

By zooming in the low energy range of the TA spectra, we observe a broad bleach feature centered at about 630 nm. This feature, previously attributed to the CT state is shown in Fig. S14 in the TA spectra recorded at slightly higher excitation fluency than for the other experiments (about twice higher).

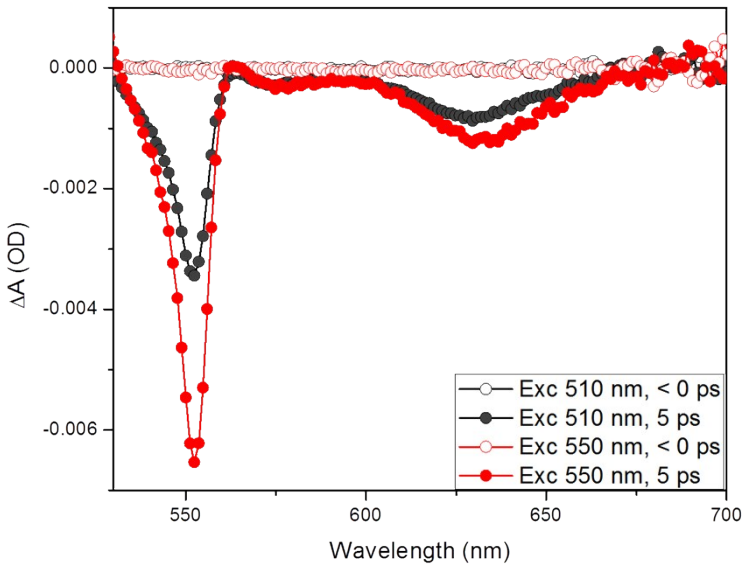

Figure S14. Zoom of the TA spectra of sample 1 after excitation at 510 nm (HX CdSe, in black) and 550 nm (HX CdTe, in red). The TA spectra at negative time are shown for comparison (white filled circles).

The dynamics of sample 2 and 3 for the different excitation wavelengths are presented in Fig. S15 and Fig. S16, respectively.

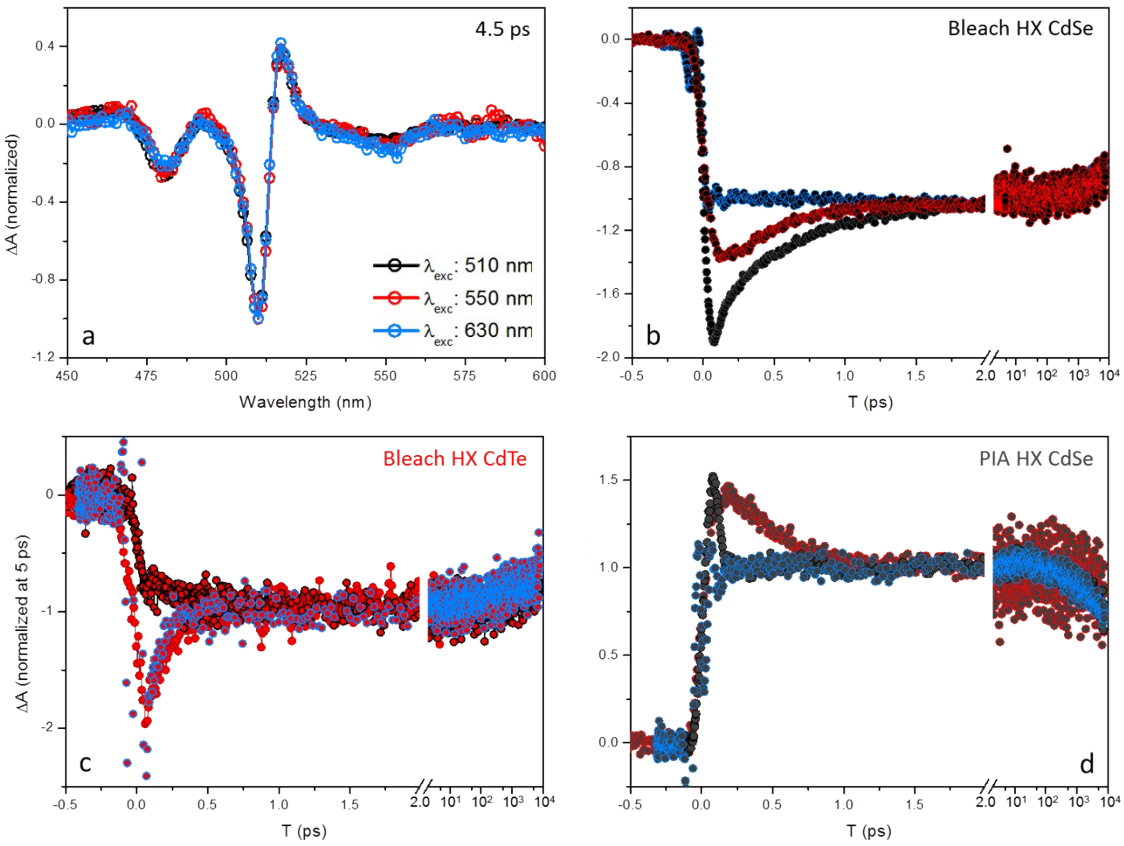

Figure S15 a. Normalized TA spectra of CdSe-CdTe NPLs (sample 2) at 4.5 ps (left) for the three different excitation wavelengths: 510 nm (HX CdSe, in black), 550 nm (HX CdTe, in red) and 630 nm (in blue). b,c,d. Dynamics of the corresponding bleach and PIA features normalized at 4.5 ps.

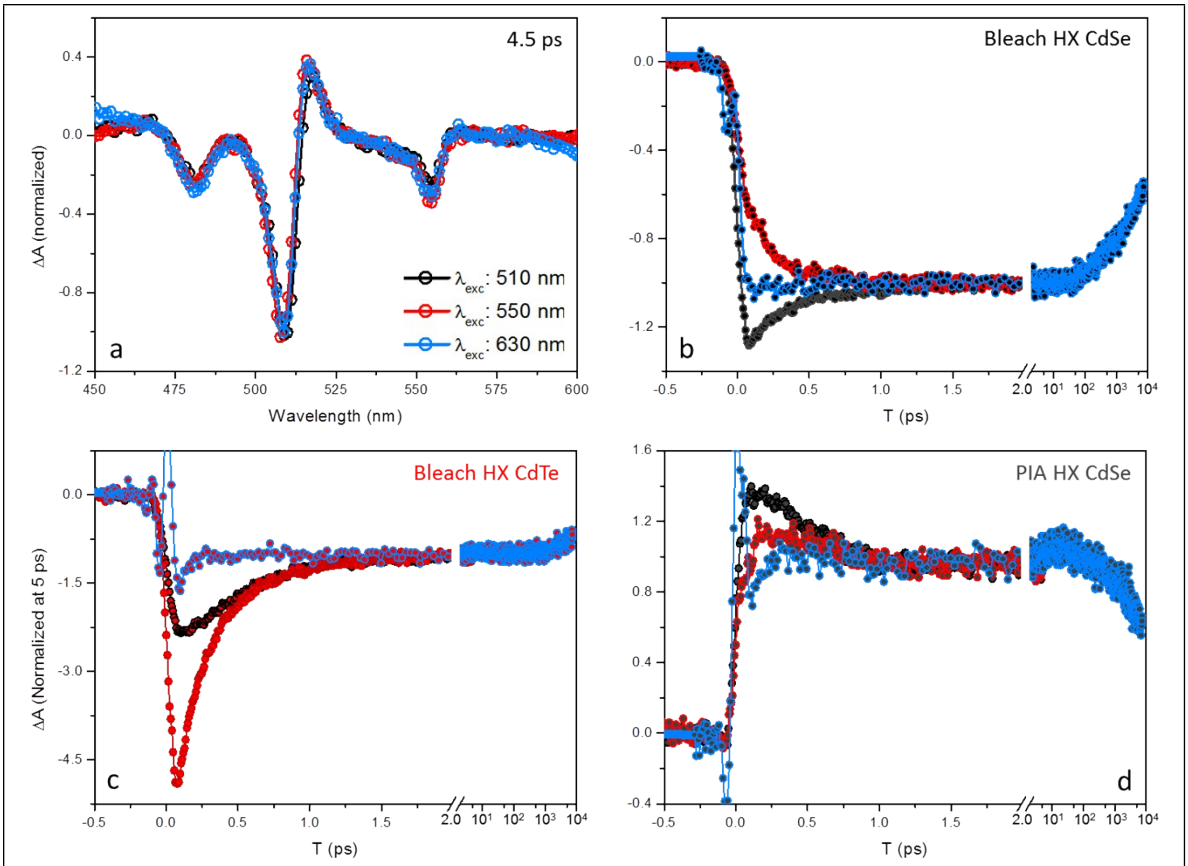

Figure S16 a. Normalized TA spectra of CdSe-CdTe NPLs (sample 3) at 4.5 ps (left) for the three different excitation wavelengths: 510 nm (HX CdSe, in black), 550 nm (HX CdTe, in red) and 630 nm (in blue). b,c,d. Dynamics of the corresponding bleach and PIA features normalized at 4.5 ps.

We also measure a CdSe-CdTe NPL sample with a larger thickness (sample 5, 5.5 MLs in thickness). The TA spectra and dynamics are shown in Fig. S17.

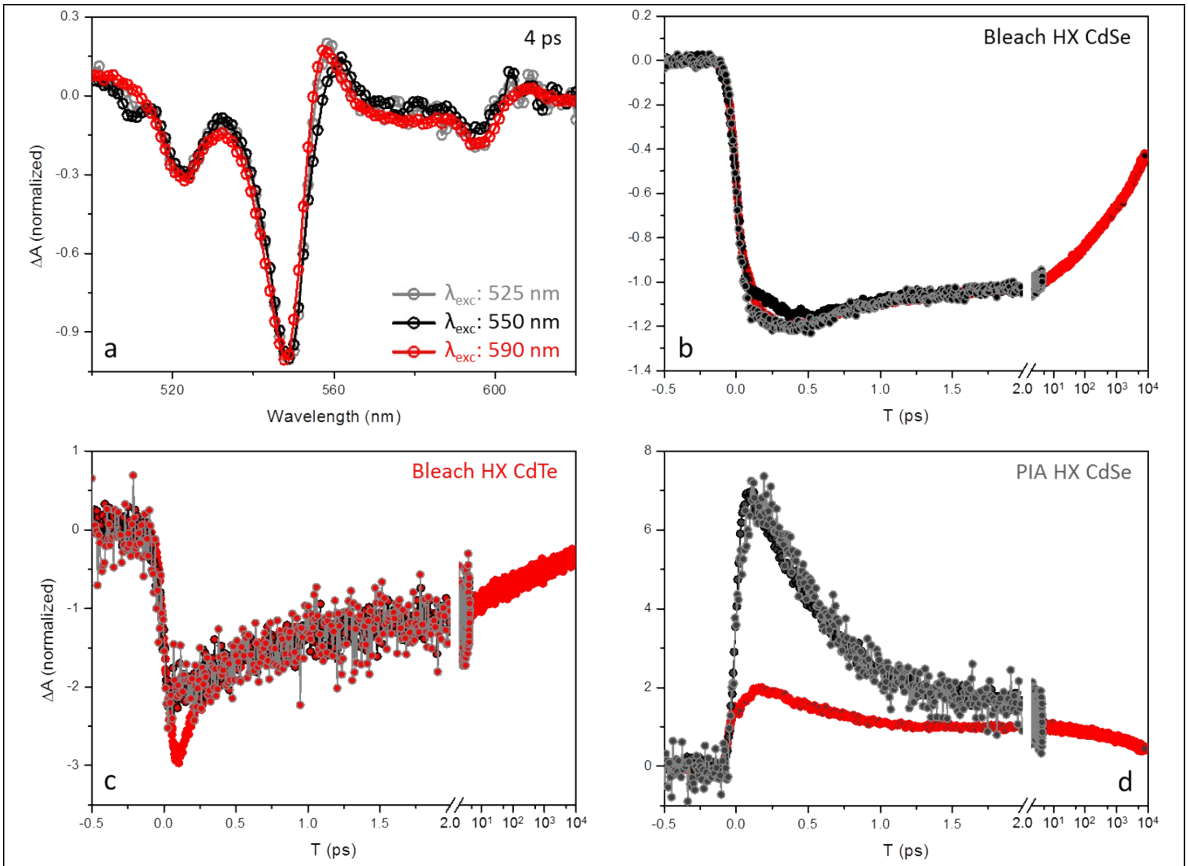

Figure S17. a. Normalized TA spectra of CdSe-CdTe NPLs with 5.5 MLs (sample 5) at 4 ps, for excitation in LX CdSe (grey), HX CdSe (black) and HX CdTe (red). b, c, d. Corresponding dynamics of the different features.

12. Simulation of transient absorption spectrum

Here we simulate a transient absorption spectrum of CdSe-CdTe NPLs when excited at 550 nm corresponding to HX CdTe optical transition. Starting from the well separated excitonic transitions in the linear spectrum (lorentzian lineshapes, fixed linewidth and initial position), we simulate a differential spectrum resulting from a peak shift (Stark effect) or a change of optical density (bleached transitions). The results for one pump-probe delay time are presented in Fig. S18. The spectrum in blue was simulated by only considering a spectral shift in the CdSe optical transitions (bleach and shift for CdTe transitions). The red TA spectrum was however simulated by considering both a spectral shift and a bleach in the CdSe optical transitions. By comparing to the experimental spectrum, we clearly see that the excitation in HX CdTe induces a bleach feature at 510 nm and 480 nm that cannot be induced by a spectral shift only.

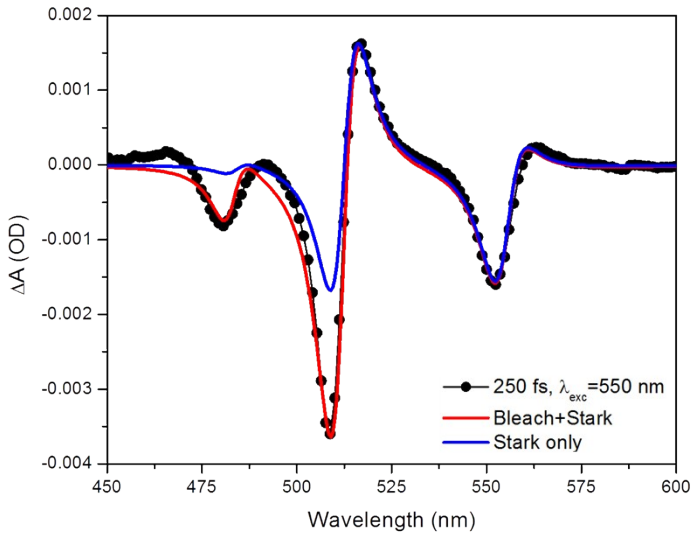

Figure S18. Simulated TA spectra of CdSe-CdTe NPLs after excitation at 550 nm. After pumping, HX and LX CdSe transitions are slightly shifted in energy due to the presence of the electron and hole in CdTe, resulting in absorption first-derivative-like feature in the TA spectrum around 480 and 510 nm (blue spectrum). If the wavefunction of the electron or hole photocreated delocalizes in CdSe, pure bleaching (< 0 only) occurs in addition to the spectral shift (red spectrum). The experimental TA spectrum of CdSe-CdTe NPL (sample 1) is shown for comparison (black dots).

13. Fit of the dynamics

To evaluate the contribution of the negative PIA signal in the bleach of a chosen transition, for each following time-resolved dynamics we superpose the opposite of the dynamics of the corresponding positive PIA feature (in a first approximation negative and positive contribution from Stark effect should be equal).

- Fit of the hole trapping in CdSe NPLs.

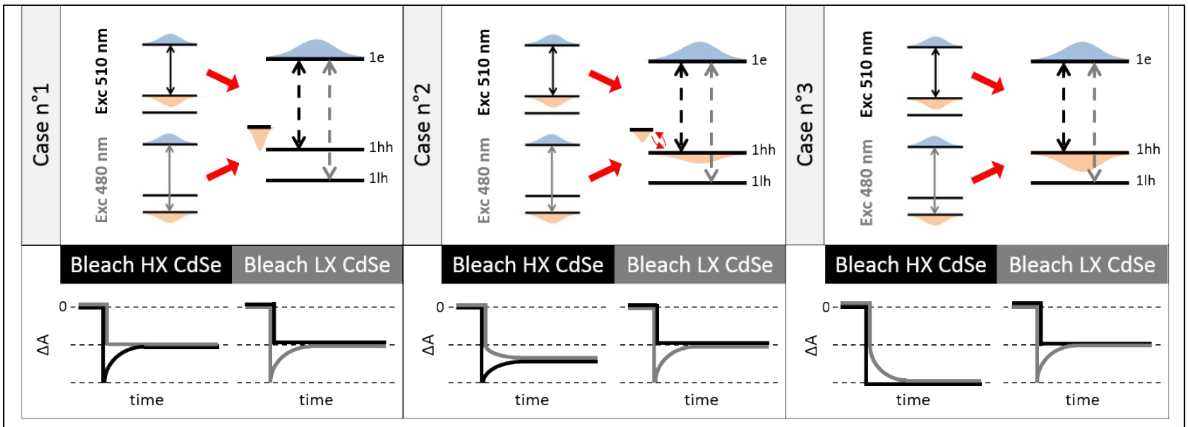

Figure S19. Model cases illustrating three different dynamics that can take place in CdSe NPLs: 1) ultrafast hole trapping (faster than the light hole to heavy hole relaxation), 2) the trapping of the hole is ultrafast but reversible at longer time scale, 3) light hole to heavy hole relaxation in the absence of hole trap states.

In Fig. S19 we illustrate by three models the possible dynamics occurring in CdSe core-only NPLs. Together, the results from the TA experiments and steady-state photoluminescence converge to the model case 2 (in the middle).

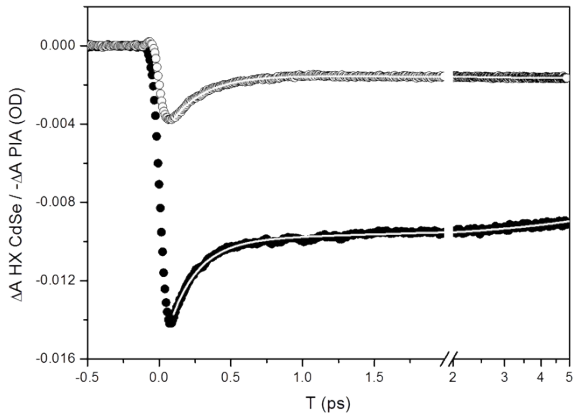

Figure S20. Dynamics of the HX CdSe bleach (black dots) and of the corresponding PIA (white dots, -ΔA) of CdSe NPLs after excitation at 510 nm. The fits are represented with a white line (fit parameters displayed below).

The fit of the HX CdSe bleach of CdSe NPL after excitation at 510 nm give a decay time constant of 193 ± 3 fs (39 %) and 48.5 ± 0.7 ps (61 %).

- Fit of the hole transfert (trapping) in CdSe-CdTe NPLs

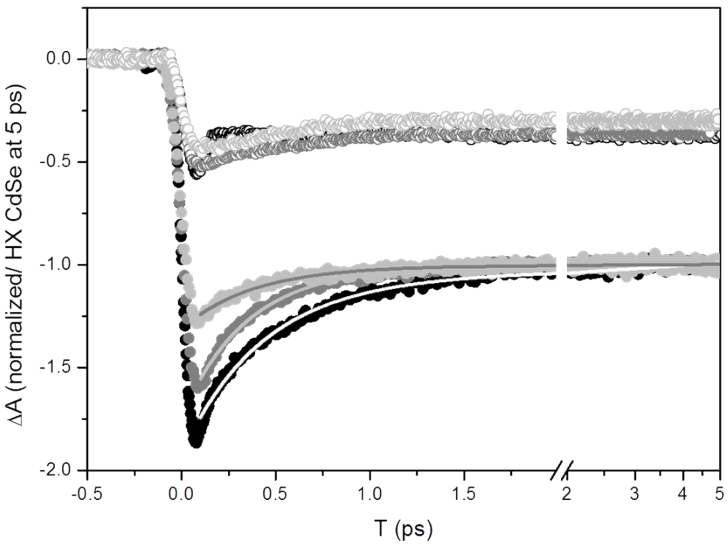

Figure S21. Early time dynamics of HX CdSe bleach normalized at 5 ps (left, full dark to grey dots) when exciting at 510 nm for three different CdSe-CdTe NPL samples (from dark to light color: sample 2, sample 1, sample 3) with their corresponding fit (continuous line). The relative positive PIA signal is flipped in sign and shown for comparison (-ΔA, open circles of the corresponding color). Fit parameters for HX CdSe can be found in Table S7.

The fit parameters of the HX CdSe bleach decay are shown in Table S7.

	$y_0 + A_1\, exp(-T/t_1)$	
	$\frac{A_1}{A_1 + y_0}$	t_1
Sample 2	45 %	428 ± 9 fs
Sample 1	42 %	344 ± 4 fs
Sample 3	23 %	377 ± 15 fs

Table S7. Parameters used to fit the bleach feature of HX CdSe after pumping at 510 nm.

- Fit of the hole transfer in CdSe-CdTeSe NPLs

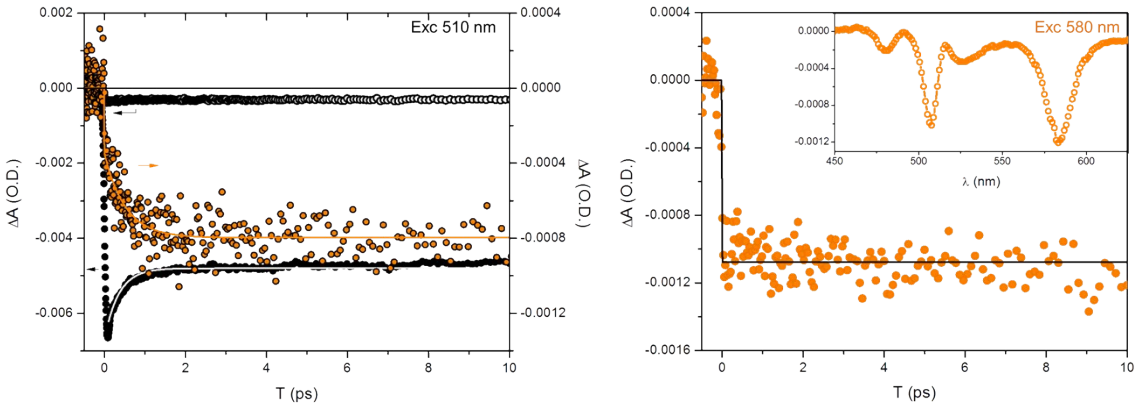

Fig. S22. Left: early time dynamics of HX CdSe (black dots) and HX CdTeSe (orange dots) bleaches after excitation at 510 nm in CdSe-CdTeSe NPLs (sample 4). The signal of the PIA of HX CdSe is shown for comparison (white filled dots). Right: Dynamics of HX CdTeSe bleach after excitation at 580 nm. The TA spectrum at T = 4.5 ps is shown in inset. Full lines represent the fit of the dynamics (parameters displayed below).

The hole transfer from CdSe to CdTeSe can be visualised in Fig. S22 (left) with the decay of the HX CdSe bleach (fitted time constant 349 ± 8 fs, amplitude 28%) after excitation at 510 nm and the corresponding growth of HX CdTeSe (fitted time constant 485 ± 83 fs, plus 57 % in amplitude). The mismatch between the two time constants can results from the weaker fit accuracy of the HX CdTeSe bleach dynamics due to the presence of a higher noise level. The absence of decay in the first 10 ps of the HX CdTeSe bleach after direct excitation (580 nm, Fig. S22 right) evidences the absence of hole trapping in this Cdse-CdTeSe NPL sample.

References:

[1] S. Ithurria, M.D. Tessier, B. Mahler, R.P.S.M. Lobo, B. Dubertret and Al. L. Efros, *Nature Materials*, 2011, **10**, 936-941.

[2] S. Pedetti, S. Ithurria, H. Heuclin, G. Patriarche and B. Dubertret, *J. of Am. Chem. Soc.*, 2014, **136**, 16430-16438.

[3] D.B. Turner, K.E. Wilk, P.M.G. Curmi and G.D. Scholes, *J. Phys. Chem. Lett.*, 2011, **2**, 1904-1911.

[4] S. Akturk, M. Kimmel, P. O'Shea and R. Trebino, Opt. Express., 2003, 11, 68-78.

[5] J.J. Snellenburg, S.P. Laptenok, R. Seger, K.M. Mullen, I.H.M. van Stokkum, *J. of Stat. Soft.*, 2012, **49**, 3.

[6] E. Cassette, R.D. Pensack, B. Mahler and G.D. Scholes, *Nature Commun.*, 2015, **6**:6086.